Article type	Case report
Article no.	AMJSPORTS/2007/047415
Title	Biomechanics of supination ankle sprain – a case report of an accidental injury event in the laboratory
Running title	Biomechanics of supination ankle sprain
Keywords	Anterior talofibular ligament, inversion, cutting motion, kinematics, plantar pressure

INTRODUCTION

Ankle sprain is the most common injury in sports (Fong et al., 2007), but the mechanism of injury is not clear. Injury mechanisms can be studied through many different approaches (Krosshaug et al., 2005). Over the years, ankle kinematics has been studied during simulated sub-injury or close-to-injury situations, i.e., sudden simulated ankle spraining motion on inversion platforms (Myers et al., 2003). Since these tests did not induce real injury, they could only somewhat suggest the ankle kinematics during an ankle sprain injury. The most direct way is to investigate real injuries using biomechanical measuring techniques. However, it is obviously un-ethical to do experiments where test subjects are purposefully injured. Nevertheless, in rare cases accidents may occur during biomechanical testing (Barone et al, 1999; Zernicke et al, 1977). It has been shown that video sequences from sports competitions can provide limited but valuable information for qualitative ankle injury analysis (Andersen et al., 2004). However, quantitative biomechanics analysis of sport injury is not easy as it requires calibrated multi-view video sequences. This study presented an accidental supination ankle sprain injury occurred in a laboratory under a high-speed video and plantar pressure capturing setting.

CASE REPORT

The injury case

One male athlete (age = 23 years, height = 1.75m, body mass = 62.6kg) wore a pair of high-top basketball shoes and performed a series of cutting motion trials in a laboratory. The university ethics committee approved the study. The subject was instructed to run forward for six meters with maximum speed, before making a rapid left turn within the capture volume. In the fourth trial, the athlete accidentally sprained his right ankle. The injury was immediately diagnosed as a grade one mild anterior talofibular ligamentous (ATFL) sprain by a well-trained orthopaedic specialist with the Jackson grading system (1974), as the athlete had pain and tenderness during palpation on ATFL with an applied supination motion, and had a mild or no functional loss, limp, swelling and point tenderness at the injured ankle. Calcaneofibular ligament and syndesmotic involvement were ruled out as there was no tenderness of these structures during the reproduction of an ankle supination by the examiner. Ankle instability was not observed during anterior drawer and talar tilt tests. Prior to the current injury, the athlete had normal foot structure with no pain, symptoms or limitation of foot and ankle function, and did not have a history of ankle sprain or other ankle injury in the previous three years. After the injury, he suffered from pain and tenderness for two weeks, and returned to full activity in three weeks, without non-weight bearing for any period.

Marker-based motion analysis of the injury mechanism

The injury motion was videotaped by three synchronized and calibrated high-speed cameras, operating on 100 Hz (JVC 9600, Japan). The shutter speed was 1/250s and the effective capture volume was about $1m^3$. The plantar pressure and the excursion path of the center of pressure were also simultaneously recorded at 100 Hz by a pressure insole system (Novel Pedar, Germany). The moment of foot strike on the ground was identified by the plantar pressure data. Part of the video sequence from the three cameras is shown in Figure 1 (in every 0.08s), and the videos are provided online at the AJSM website at http://ajs.sagepub.com. The positions of the tibia tuberosity, the lateral malleolus, the proximal posterior shank, the distal posterior shank, the proximal heel, the distal heel and the toe tip were manually digitized with a motion analysis system (Ariel Performance Analysis System, USA). The digitizing process was done ten times by the same researcher to obtain the average values of the coordinates of the anatomical landmarks.

A static standing calibration trial in the anatomical position served as the offset position to determine the segment embedded axes of the shank and foot. For this recording, we also digitized the lateral femoral condyle. Axis transformations were performed to make the vertical axes of the shank (X3) passes through the knee and ankle joint centers. The joint center of the knee was determined by the method of Davis and co-workers (1991), and the ankle joint center location was defined 1 cm distal to the lateral malleolus, as proposed by Eng and Winter (1995). The antero-posterior axis (X1) of the local axis system was defined perpendicular to the X3 axis with no medio-lateral component. The third axis was the cross product of the vertical and antero-posterior axis (X2 = X3 x X1). The axes of the foot were aligned with the global coordinate system. The method of Soderkvist and Wedin (1993) was utilized to obtain the segment embedded reference frame for the shank, using the tibia tuberositas, the lateral malleolus, the proximal posterior shank and the distal posterior shank markers. Smoothing and interpolation were performed by the generalized cross validation package of Woltring (1986). The cubic mode with an 8 Hz cut-off frequency was chosen for the marker trajectories. The joint angles presented here were calculated using the method described by the ISB recommendation committee (Wu et al., 2002). Ankle angles and angular velocities are presented in the three orthogonal anatomical planes (Inversion/eversion about the X1 axis; plantarflexion/dorsiflexion about the X2 axis; internal/external rotation about the X3 axis). The calculations were done using customized Matlab scripts.

Validation of the ankle kinematics of the injury trial

To validate the measured kinematics, the injury video sequences were also analyzed using the model-based image-matching (MBIM) technique described by Krosshaug and Bahr (2005). Models of the surroundings were manually matched to the calibration cube frame (50x50x50cm) and lines on the floor in every camera view from calibration trial video, by adjusting the camera calibration parameters (position, orientation and focal length). A skeleton model (Zygote Media Group Inc., Provo, Utah, USA) was customized to match the anthropometry of the injured subject. The skeleton matching started with the thigh segment. We thereafter worked distally by matching the shank, feet and toe segments. In contrast to previous work where axial rotation was evenly distributed between the knee and ankle, we chose to distribute the axial rotation solely to the ankle as it was considered more likely due to the injury loads. The joint angle time histories were read into Matlab with a customized script for data processing. To allow direct comparisons between the marker-based measurements and the MBIM technique, the axis systems of the skeleton model were re-aligned as outlined in Krosshaug and Bahr (2005). The ankle kinematics reported by both methods is shown in Figure 2. The patterns were generally in good agreement, as shown by similar shapes and ranges of motion. Therefore, validation was considered achieved.

Kinematics comparison of the injury trial and the normal trials

The same procedure of the marker-based motion analysis was performed for the three successful normal trials before the injury trial for comparison. Figure 3 shows the ankle angles and the angular velocities for the successful normal trials and the injury trial. At foot strike, for the injury trial, the ankle was 7 degrees more internally rotated (less externally rotated from 21 to 14 degrees) and 6 degrees more inverted (from 9 to 15 degrees) when compared to the normal trials (Table 1). After landing, there was a two-phase change of ankle kinematics, as primarily determined by the profile changes of inversion and inversion velocity. Firstly, from 0.06s, the ankle entered a pre-injury phase (Phase I) as the kinematics profile started to deviate from that of normal trials, as shown by a larger inversion, accompanied by greater plantarflexion velocity and internal rotational velocity. The change of inversion in this period was still gentle, as the inversion velocity did not differ much from that of normal trials. Therefore this period is termed “pre-injury phase” as we believed that the injury had not occurred yet, however, a significant risk may have been developed. At 0.11s, the deviation halted and the ankle was inverted for 32 degrees, externally rotated for 5 degrees and dorsiflexed for 14 degrees. Secondly, from 0.11s onwards, the ankle entered the injury phase (Phase II), as there was another explosive inversion and internal rotation shown

by the increased velocities. The ankle further inverted for 16 degrees and internally rotated for 15 degrees. At 0.20s, the ankle reached its greatest angular displacement from the offset anatomical position. The orientation was at an absolute measure of 48 degrees inversion, 10 degrees internal rotation, and 18 degree dorsiflexion.

Plantar pressure analysis of the injury trial and the normal trials

The plantar pressure distributions of one selected normal trial and the injury trial are provided online at the AJSM website at http://ajs.sagepub.com. The hallux was found to contribute to greater contact with the ground during most of the stance, especially in normal trials. For the injury trial, higher pressure at both heel and forefoot region was found at 0.02s after the foot strike, indicating a firm and forceful foot strike. At 0.06s onwards, the pressure at heel reduced quickly and shifted to the forefoot region. Such pattern suggested a lift of the rearfoot and a quick shift of center of pressure to the forefoot after foot strike, from 0.02 to 0.08s, as also shown by a quick move of the center of pressure from heel to mid-foot region in Figure 4. From 0.08s to 0.20s, a chaotic pattern of the center of pressure excursion at the third and fourth metatarsal region was found, indicating an unstable foot support during this period. After 0.24s, the center of pressure shifted forward to the proximal third metartarsal, and further to the first metartarsal region finally. In normal trials, the excursion path of the center of pressure moved progressively from heel to metatarsal region in a rather stable manner.

DISCUSSION

For the successful normal trials, the ankle was externally rotated and slightly inverted at foot strike. Such orientation enhanced a flat foot landing with a maximum contact surface between the foot and the ground. For the injury case, the ankle was more internally rotated (or less externally rotated) at foot strike – this was suggested to be a vulnerable orientation for sustaining ankle sprain injury (Andersen et al., 2004). However, in contrast to the hypotheses in previous studies, dorsiflexion instead of plantarflexion was found. In fact, when we retrieved Figure 3-D from Andersen's study (2004), we found that the ankle may be in a dorsiflexed orientation too. Therefore the previous belief that the ankle is plantarflexed during a sprain injury may not be essential. In this case report, right after landing, the dorsiflexed ankle started plantarflexing in 0.06s, shifted the center of pressure to forefoot and lifted the rearfoot. While the forefoot was in touch with the ground and supported the body, the rearfoot drifted to the lateral side – this was a pivoting internal rotational motion. Such motion swung the ankle joint center to the lateral aspect and deviated it from the application point of the ground reaction force, as indicated by the center of pressure position. A laterally shifted center of pressure was suggested to be a risk factor to sustain ankle

sprain injury (Willems et al, 2005), and thus may have predisposed the ankle at a high risk to sustain a sprain. It was also speculated that the pivoting internal rotational motion resulted in a longer moment arm along the ankle joint. As the moment, or torque, is the product of the ground reaction force and the moment arm, it should have increased greatly as a result (Wright et al., 2000). Therefore, the lift and the lateral swing of the rearfoot may contribute to a sudden explosive torque and the subsequent abrupt kinematics changes at the ankle joint.

The changes of ankle kinematics were in a two-phase pattern. In the pre-injury phase, the ankle orientation was within the normal ankle motion range (Hertel, 2002). Therefore, it was postulated that the ATFL sprain injury had not been induced yet in this phase. However, after this phase, at 0.11s, the ankle entered an at-risk orientation – an internally rotated and inverted position (Andersen et al., 2004), which may lead to the second injury phase that sprained the ATFL. At the lateral aspect of ankle, the peroneal muscles play a role to pronate the foot, which oppose the supination or inversion motion. Previous myoelectric investigation suggested that the reaction time of peroneal muscles in healthy male subjects with stable ankles was 55-80ms (Konradsen and Ravn, 1991), and an inactive peroneus may be the reason why the sprain occurred. Therefore, in the current case report, we believed that the peroneal muscles were not yet activated before the start of the pre-injury phase, that is, at 0.06s, to protect the ankle joint from going into the second injury phase at 0.11s. During this period, sudden inversion and internal rotation were observed, which reflected how the explosive ankle supination torque introduced the grade one ATFL sprain injury.

This study provides information for understanding the ankle sprain mechanism quantitatively. Previous cadaveric and simulation studies may have involved too much plantarflexion and thus may not reflect the real ankle joint biomechanics during real injury. Future studies should be planned to incorporate post-injury video analysis with the model-based image-matching (MBIM) technique (Krosshaug and Bahr, 2005) to better understand the ankle kinematics during real injury scenarios.

SUMMARY

This study presented the biomechanics of an accidental supination ankle sprain injury. At injury, the ankle reached an inversion of 48 degrees, accompanied by an internal rotation of 10 degrees. However, in contrast to the hypotheses in previous studies, dorsiflexion instead of plantarflexion was found at injury. The findings of this study add knowledge to the current understanding of ankle sprain mechanism and raise a

debate on the ankle joint orientation during an inversion sprain injury. This reveals the need to conduct systematic post-injury video analysis on real injury scenarios. The findings may also provide valuable information for designing prophylactic device for ankle sprain prevention.

REFERENCES

Andersen, T.E., Floerenes, T.W., Arnason, A., Bahr, R. Video analysis of the mechanisms for ankle injuries in football. American Journal of Sports Medicine, 2004;32(1 Suppl), S69-S79.

Barone, M., Senner, V., Schaff, P. ACL injury mechanism in alpine skiing: analysis of an accidental ACL rupture. In: R.J. Johnson (Eds.), Skiing Trauma and Safety, 1999:12, 63-81. West Conshohocken PA: American Society for Testing and Materials.

Davis, R.B., Ounpuu, S., Tyburski, D., Gage, J.R., A gait analysis data collection and reduction technique. Human Movement Science, 1991;10(5), 575-578.

Eng, J.J. Winter, D.A. Kinetic analysis of the lower limbs during walking: what information can be gained from a three-dimensional model? Journal of Biomechanics, 1995;28(6), 753-758.

Fong, D.T.P., Hong, Y., Chan, L.K., Yung, P.S.H., Chan, K.M. A systematic review on ankle injury and ankle sprain in sports. Sports Medicine, 2007;37(1), 73-94.

Hertel, J. Functional anatomy, pathomechanics, and pathophysiology of lateral ankle instability. Journal of Athletic Training, 2002;37(4), 364-375.

Jackson, D.W., Ashley, R.L., Powell, J.W. (1974). Ankle sprains in young athletes. Relation of severity and disability. Clinical Orthopaedics and Related Research, (101), 201-215.

Konradsen, L., Ravn, J.B. Prolonged peroneal reaction time in ankle instability. International Journal of Sports Medicine, 1991;12(3), 290-292.

Krosshaug, T., Andersen, T.E., Olsen, O.E., Myklebust, G., Bahr, R. Research approaches to describe the mechanisms of injuries in sport: limitations and possibilities. British Journal of Sports Medicine, 2005:39(6), 330-339.

Krosshaug, T., Bahr, R. A model-based image-matching technique for three-dimensional reconstruction of human motion from uncalibrated video sequences. Journal of Biomechanics, 2005;38(4), 919-929.

Myers, J.B., Riemann, B.L., Hwang, J.H., Fu, F.H., Lephart, S.M. Effect of peripheral afferent alteration of the lateral ankle ligaments on dynamic stability. American Journal of Sports Medicine, 2003;31(4), 498-506.

Soderkvist, I., Wedin, P.A. Determining the movements of the skeleton using well-configured markers. Journal of Biomechanics, 1993;26(12), 1473-1477.

Woltring, H.J. A Fortran package for generalized, cross-validatory spline smoothing and differentiation. Advances in Engineering Software, 1986;8(2), 104-113.

Willems, T., Witvrouw, E., Delbaere, K., De Cock, A., De Clercq, D. Relationship between gait biomechanics and inversion sprains: a prospective study of risk factors. Gait and Posture, 2005;21(4), 379-387.

Wright, I.C., Neptune, R.R., van den Bogert, A.J., Nigg, B.M. The influence of foot positioning on ankle sprains. Journal of Biomechanics, 2000;33(5), 513-519.

Wu, G. Siegler, S., Allard, P., Kirtley, C., Leardini, A., Rosenbaum, D., Whittle, M., D'Lima, D.D., Cristofolini, L., Witte, H., Schmid, O., Stokes, I. ISB recommendation on definitions of joint coordinate system of various joints for the reporting of human joint motion – Part I: ankle, hip, and spine. Journal of Biomechanics, 2002;35(4), 543-548.

FIGURE LEGENDS

Figure 1 – The video sequence (in every 0.08s) of the supination ankle sprain injury with the matched skeleton model

Figure 2 – The ankle kinematics reported by the marker-based and the Poser motion analysis methods

Figure 3 – Ankle angle and angular velocity among the three axes for the successful normal trials (3 trials) and the injury trial (1 trial)

Figure 4 – The excursion path of the center of pressure of (a) the mean of the normal trials, and (2) the injury trial

Table 1 – Ankle orientation at foot strike and the maximum ankle angular displacement during stance for the normal trials and the injury trial

	Normal trials (N = 3)	Injury trial (N = 1)	
At Foot Strike			
Plantarflexion / Dorsiflexion	-14 deg*	-11 deg*	
Internal / External rotation	-21 deg*	-14 deg*	
Inversion / Eversion	9 deg	15 deg	
During Stance		Phase I	Phase II
Max plantarflexion	15 deg	1 deg	-15 deg*
Max internal rotation	-6 deg*	-5 deg*	10 deg
Max inversion	35 deg	41 deg	48 deg
Max plantarflexion velocity	730 deg/s	370 deg/s	93 deg/s
Max internal rotation velocity	320 deg/s	138 deg/s	271 deg/s
Max inversion velocity	638 deg/s	632 deg/s	272 deg/s

Note: * Negative value means dorsiflexion and external rotation respectively. Phase I = Pre-injury Phase, from 0.06 to 0.11s. Phase II = Injury Phase, from 0.11s onwards.

Figure 1. The video sequence (at 0.08 second intervals) of the supination ankle sprain injury with the matched skeleton model.

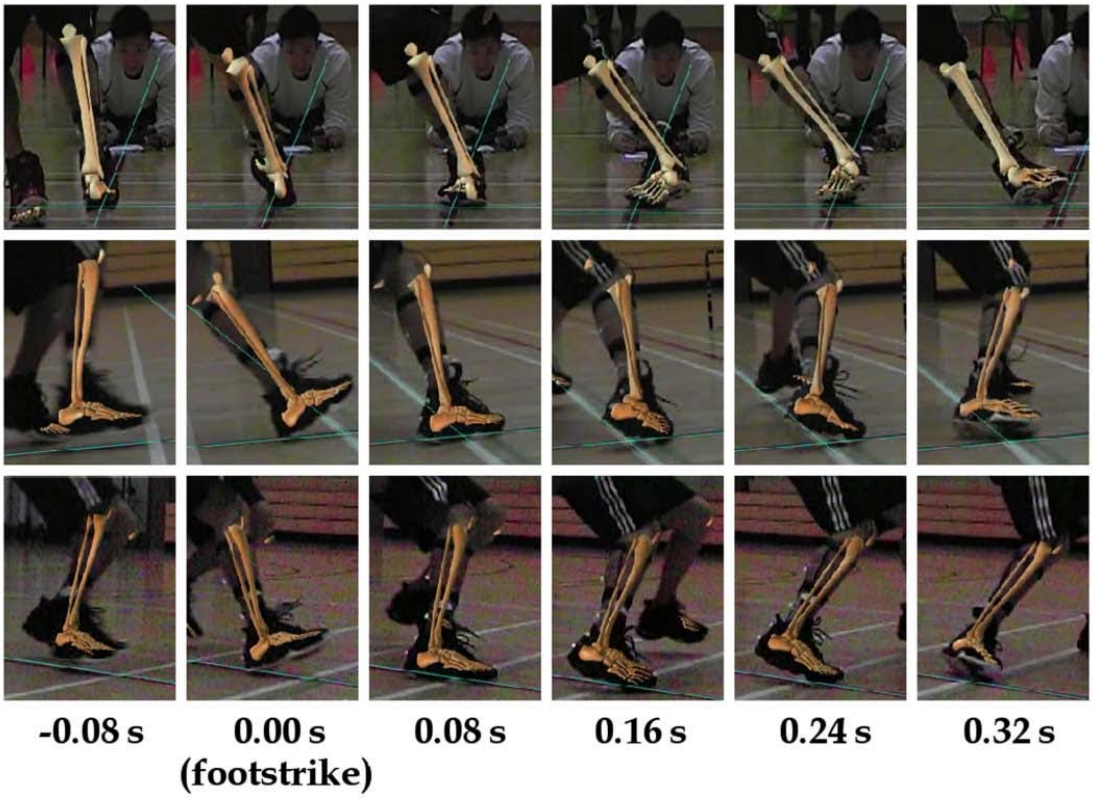

Figure 2. The ankle kinematics reported by the marker-based (A) and the model-based (B) image-matching (MBIM) motion analysis methods.

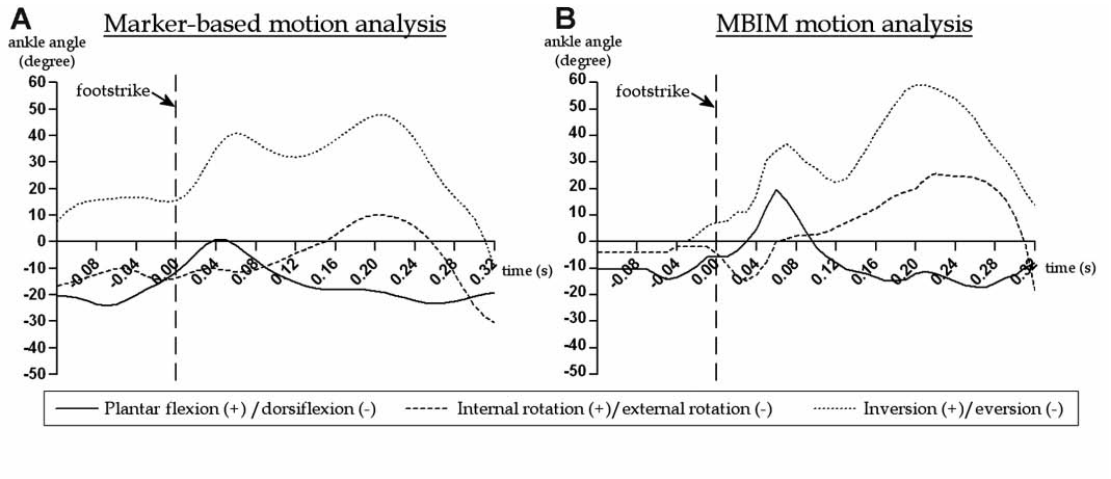

Figure 3. Ankle angle (A) and angular velocity (B) among the 3 axes for the successful normal trials (3 trials) and the injury trial (1 trial).

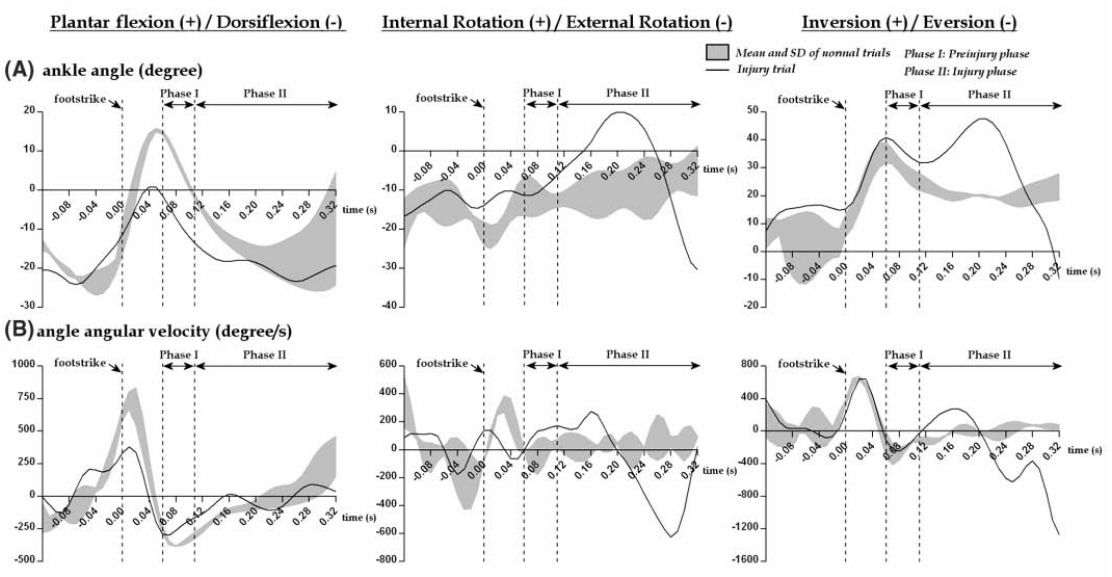

Figure 4. The excursion path of the center of pressure of the mean of the normal trials (A) and the injury trial (B).